Sun et al. Nanoscale Research Letters (2017) 12:224
DOI 10.1186/s11671-017-2003-2

Nanoscale Research Letters

NANO EXPRESS Open Access

Absorption Amelioration of Amorphous Si Film by Introducing Metal Silicide Nanoparticles

Hui Sun[1], Hsuan-Chung Wu[2], Sheng-Chi Chen[2,3*], Che-Wei Ma Lee[2] and Xin Wang[1]

Abstract

Amorphous Si (a-Si) films with metal silicide are expected to enhance the absorption ability of pure a-Si films. In this present study, NiSi (20 nm)/Si (40 nm) and AlSi (20 nm)/Si (40 nm) bilayer thin films are deposited through radio frequency (RF) sputtering at room temperature. The influence of the film's composition and the annealing temperature on the film's optical absorption is investigated. The results show that all the NiSi/Si films and AlSi/Si films possess higher absorption ability compared to a pure a-Si film (60 nm). After annealing from 400 to 600 °C under vacuum for 1 h, the Si layer remains amorphous in both NiSi/Si films and AlSi/Si films, while the NiSi layer crystallizes into $NiSi_2$ phase, whereas Al atoms diffuse through the whole film during the annealing process. Consequently, with increasing the annealing temperature, the optical absorption of NiSi/Si films increases, while that of AlSi/Si films obviously degrades.

Keywords: Absorption ability, Metal silicide, Amorphous silicon, RF sputtering

Background

So far, a great deal of research has been done on the development of alternative energies, such as solar energy, since fossil fuels are non-renewable [1–3]. Among the device types of photovoltaic cells, much effort has been put into the thin film solar cells due to their flexible feature, low cost, light weights, etc. [4–6]. As for the film material, amorphous silicon (a-Si) is one of the most popular candidates [7–13]. Their abundance, non-toxicity, low manufacturing cost, uniformity over large areas, and adaptability to various substrates have attracted considerable interest [14, 15]. However, the significant recombination of photo-generate carriers, and the light-induced degradation derived from the Staebler-Wronski effect limit the widespread use of a-Si in photovoltaic applications [16–18]. Decreasing the film's thickness is an effective solution to solve these problems [19, 20]. But unfortunately, the thinner film will possess a low optical absorption and the photoelectric conversion efficiency is also suppressed.

In order to enhance the optical absorption of a-Si thin film, many approaches have been explored, for instance, the introduction of metallic nanoparticles [21–23], dielectric nanopillars [24], and addition antireflection coatings [25, 26]. Sachan et al. demonstrated a strategy of embedding metal silicide nanoparticles into an ultrathin a-Si film [27]. The optical absorption was found to be greatly improved in the visible range (350–750 nm). Brahmi et al. also reported that silicide films exhibit high absorption coefficient in the range of 5×10^5–10×10^5 cm^{-1} in the visible light region, even though their thickness is ultrathin (~10 nm) [28].

In this work, we have introduced Ni and Al into an a-Si thin film so as to embed Ni silicide or Al silicide in the Si film. The influence of metal (Ni or Al) content on the film's optical behavior is investigated. The effect of annealing temperature on the film's microstructure and optical properties is also discussed.

Methods

a-Si thin films with Ni silicide or Al silicide were deposited by radio frequency sputtering on glass and silicon

* Correspondence: chensc@mail.mcut.edu.tw
[2]Department of Materials Engineering and Center for Thin Film Technologies and Applications, Ming Chi University of Technology, Taipei 243, Taiwan
[3]Department of Electronic Engineering, Chang Gung University, Taoyuan 333, Taiwan
Full list of author information is available at the end of the article

Table 1 Nomenclature for Ni silicide or Al silicide nanoparticle-embedded Si thin films

Composition	NS-1	NS-2	NS-3	AS-1	AS-2	AS-3
Si (at.%)	45	56	71	42	52	69
Ni (at.%)	55	44	29	–	–	–
Al (at.%)	–	–	–	58	48	31

substrates at room temperature. Firstly, NiSi layers or AlSi layers were co-sputtered from the Ni target or Al target and Si target. The layer's thickness was maintained at 20 nm. The target power on Si was varied in order to adjust the film's composition (shown in Table 1). Then, a top Si layer (40 nm) was deposited over the NiSi and AlSi layers. A pure Si film with a total thickness of 60 nm was also prepared for the purpose of comparison. Finally, all the films were annealed under vacuum at 400, 500, and 600 °C for 1 h, respectively.

The film's composition was measured by JEOL JXA-8200 electron probe X-ray microanalyzer (EPMA). The phase formation was identified by Raman spectroscopy (iHR 550) with a 532-nm laser. The depth-profiling analysis was obtained by Auger electron spectroscopy (AES, ULVAC-PHI, PHI 700). The microstructures of the specimens were observed on the film's cross-section by high-resolution transmission electron microscopy (HR-TEM, JEOL JEM-2100). The film's absorption coefficient was estimated by the following equation (Eq. 1) from the film's transmittance and reflectance data, which were measured by UV-VIS spectrophotometer (JASCO-V670).

$$\alpha = \frac{1}{d} \ln\left(\frac{1-R}{T}\right) \quad (1)$$

where d is the film thickness, R and T are the optical reflectance and transmittance, respectively.

Results and Discussion

The absorption coefficient of NiSi/Si films and AlSi/Si films is shown in Fig. 1. With increasing Ni content or Al content in the films, their absorption ability is significantly enhanced in the whole visible region (400–800 nm). Especially, compared with the pure Si film, the films with Ni silicide or Al silicide possess a much higher absorption coefficient (10^4~10^5 cm^{-1}) at the wavelength above 500 nm, where the absorption of the visible light by the pure Si film is negligible. The absorption enhancement of NiSi/Si and AlSi/Si films is believed to be attributable to the plasmonic absorption by Ni silicide or Al silicide nanoparticles in an a-Si matrix [27]. These results confirm that an obvious improvement in absorption can be achieved within amorphous Si films. Additionally, with respect to the NiSi/Si film, this improvement for the AlSi/Si film is much more evident. It may be caused by the coarse-grained interface between the NiSi layer and Si layer introducing more scattering of visible light (shown in Fig. 2). In contrast, the smooth interface between the AlSi layer and Si layer is beneficial for improving the film's absorption ability. Since the band gap of amorphous silicon is about 1.7 eV, a significant light absorption of the a-Si film can be found below 730 nm, which lies within the visible light region. Thus, the absorption enhancement of NiSi/Si and AlSi/Si films can significantly improve the efficiency of PV devices based on amorphous silicon.

Figure 2 shows the cross-sectional images of NiSi/Si (NS-1) and AlSi/Si (AS-1) films. The NiSi layer or AlSi layer and the top Si layer can be clearly observed. In the high-resolution image of Fig. $2a_1$, some nanoparticles assumed to be Ni silicide are noted. They lead the microstructure of the first layer to be much coarser. However, in the AlSi/Si film, Al silicide nanoparticles are imperceptible.

The Raman spectra of the NiSi/Si film and AlSi/Si film before and after annealing under vacuum at 400, 500, and 600 °C is shown in Fig. 3a, b, respectively. Whatever the annealing temperature, the NiSi/Si film and AlSi/Si film display a pure amorphous Si structure peaked at 480 cm^{-1}. No peak near 520 cm^{-1} assigned to the

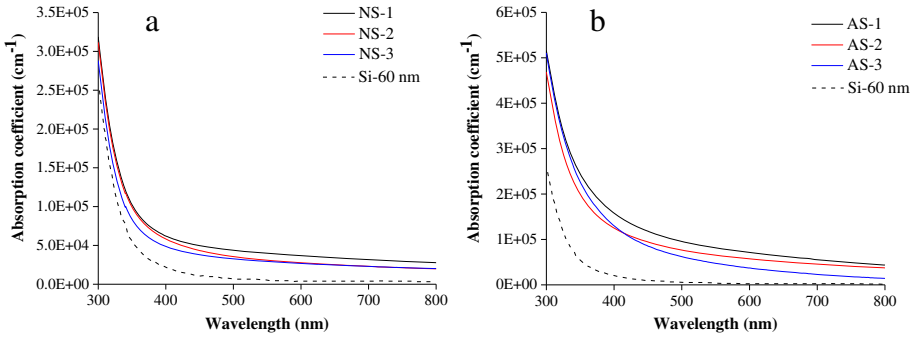

Fig. 1 The absorption coefficient of **a** NiSi/Si and **b** AlSi/Si films with various compositions

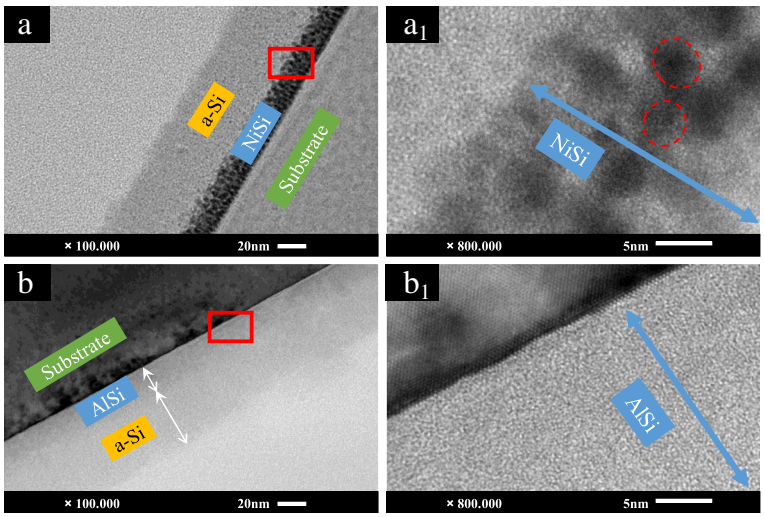

Fig. 2 The cross-sectional TEM images of **a** NiSi/Si (NS-1) and **b** AlSi/Si (AS-1) films and high-resolution images of $\mathbf{a_1}$ NiSi/Si (NS-1) and $\mathbf{b_1}$ AlSi/Si (AS-1) films derived from the areas marked with *red rectangles* in Fig. 2a, b

crystalline Si structure is detected. The absorption coefficient of NiSi/Si and AlSi/Si films annealed at different temperatures is shown in Fig. 3c, d, respectively. The absorption ability of the NiSi/Si film greatly enhances with increasing the annealing temperature, while that of AlSi/Si films gradually decreases. Since the dopants in Si are generally activated through an essential thermal annealing treatment between 400 and 1000 °C [29, 30], the degradation of the absorption ability of AlSi/Si films proves that the NiSi/Si film is more suitable for the fabrication of the absorbing layer in amorphous silicon solar cells.

The depth profiles of the atomic composition analysis of as-deposited NiSi/Si and AlSi/Si films and those films annealed at 500 °C are given in Fig. 4. After 1 h annealing under vacuum, the composition of the Si layer and

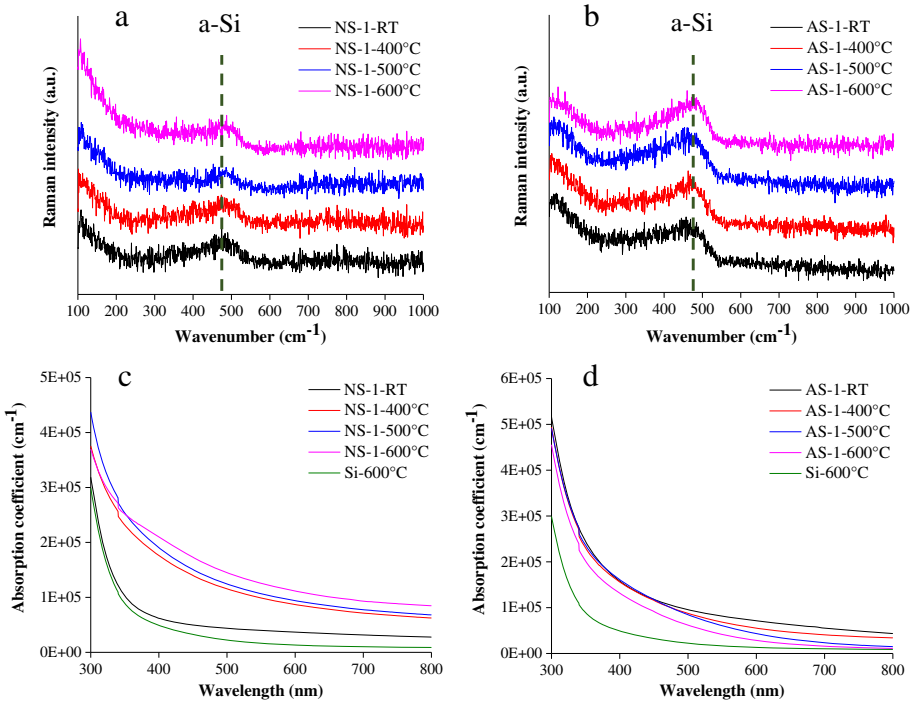

Fig. 3 Raman spectra of **a** NiSi/Si film and **b** AlSi/Si film before and after annealing in vacuum at 400, 500, and 600 °C, and the absorption coefficient of **c** NiSi/Si films and **d** AlSi/Si films annealed at different temperatures

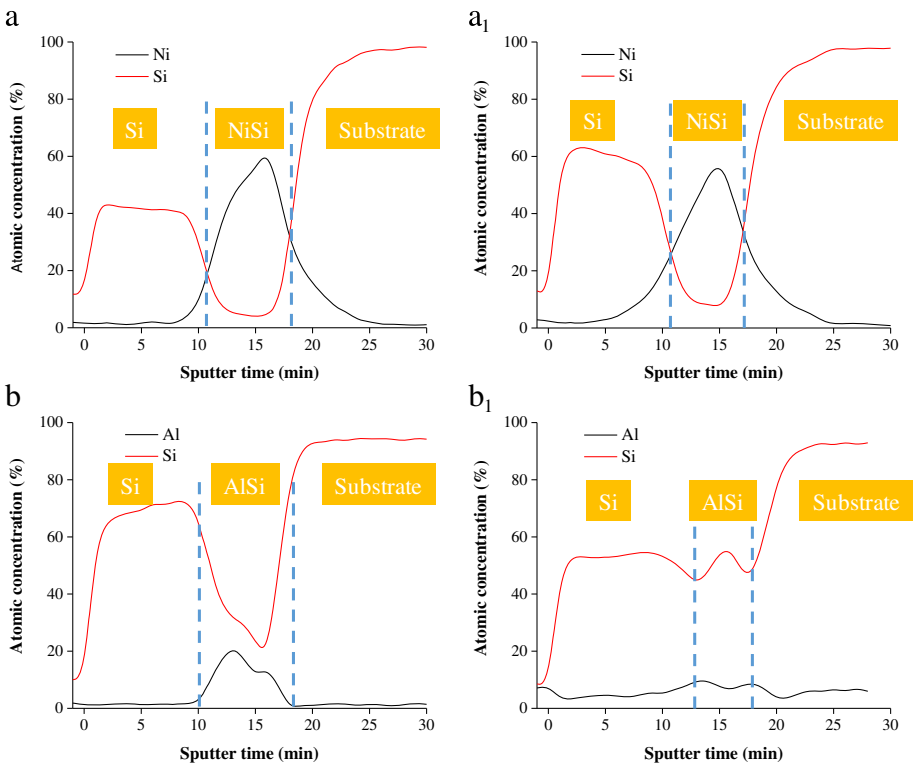

Fig. 4 The depth profile of atomic composition analysis of **a**, **b** as-deposited NiSi/Si (NS-1) and AlSi/Si (AS-1) films and $\mathbf{a_1}$, $\mathbf{b_1}$ those films annealed at 500 °C

NiSi layer remains nearly unchanged (Fig. 4a, a_1). Few nickel atoms diffuse from the NiSi layer into the adjacent Si layer. In contrast, as for the AlSi/Si film, almost all the aluminum atoms in the AlSi layer are diffused. The Al content in the AlSi layer and that in the top Si layer are close. This perhaps explains why the absorption ability of the AlSi layer is suppressed after annealing. The uniformly distributed Al clusters in the whole film reinforce the scattering and reflection of the visible light.

The cross-sectional images of NiSi/Si (NS-1) and AlSi/Si (AS-1) films annealed at 500 °C are shown in Fig. 5. Some nickel silicide nanoparticles are crystallized to

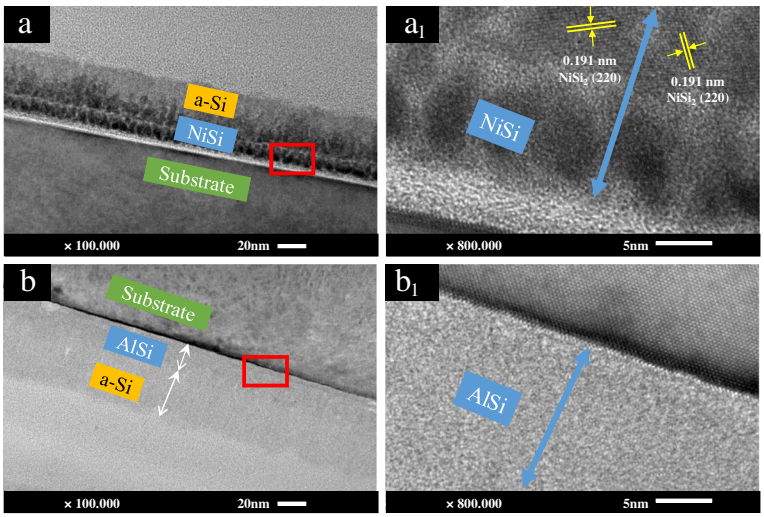

Fig. 5 The cross-sectional TEM images of **a** NiSi/Si (NS-1) and **b** AlSi/Si (AS-1) films annealed at 500 °C and high-resolution images of $\mathbf{a_1}$ NiSi/Si (NS-1) and $\mathbf{b_1}$ AlSi/Si (AS-1) films derived from the areas marked with *red rectangles* in Fig. 5a, b

form $NiSi_2$ compounds after annealing. $NiSi_2$ (220) planes with interplanar lattice spacing of 0.191 nm are identified (Fig. $5a_1$). The strengthening of absorption ability of NiSi/Si films with annealing temperature increasing can be due to the amelioration of the film's crystallinity. Besides, the interface between the AlSi layer and top a-Si layer becomes illegible after annealing (Fig. 5b). No crystallized phase can be detected (Fig. $5b_1$). This is attributed to the diffusion of aluminum atoms during the annealing process.

Conclusions

In this work, nickel silicide and aluminum silicide nanoparticles are introduced into amorphous Si thin films in order to enhance the film's absorption ability. Radio frequency sputtering was used to deposit NiSi/Si and AlSi/Si bilayer thin films. The results show that all the NiSi/Si and AlSi/Si films present an absorption improvement, especially in the long wavelength region (>500 nm), compared to the pure amorphous Si film. The as-deposited AlSi/Si films possess higher absorption compared with the NiSi/Si films. However, the AlSi/Si film's absorption ability significantly degrades after 1 h annealing under vacuum condition, which is owing to the diffusion of aluminum atoms during the annealing process, whereas the optical absorption of NiSi/Si films gradually improves after annealing. This is resulting from the enhanced crystallinity of NiSi/Si films. Our results confirm that the amorphous Si film with suitable metal silicides can expand the response to the visible light of the photovoltaic devices and improve the utilization of the solar spectrum.

Abbreviations

AES: Auger electron spectroscopy; EPMA: Electron probe X-ray microanalyzer; HR-TEM: High-resolution transmission electron microscopy; RF: Radio frequency

Acknowledgements

We gratefully acknowledge the National Natural Science Foundation of China (no. 51172217) and Ministry of Science and Technology of Taiwan (no. 103-2221-E-131-004) for their financial support. We also thank Prof. H.C. Lin and Mr. C.Y. Kao of the Instrumentation Center, National Taiwan University, for EPMA experiments.

Authors' Contributions

HS completed the experiments and drafted the manuscript. HCW and SCC designed the experiments and revised the manuscript. CWML performed the experiments and analyzed the data. XW participated in the data analysis and discussions. All authors read and approved the final manuscript.

Competing Interests

The authors declare that they have no competing interests.

Ethics Approval

We confirm that the present work did not involve endangered or protected species, and no specific permits were required for this studies.

Publisher's Note

Author details

[1]Institute of Materials Science and Engineering, Ocean University of China, Qingdao 266100, People's Republic of China. [2]Department of Materials Engineering and Center for Thin Film Technologies and Applications, Ming Chi University of Technology, Taipei 243, Taiwan. [3]Department of Electronic Engineering, Chang Gung University, Taoyuan 333, Taiwan.

Received: 20 September 2016 Accepted: 15 March 2017
Published online: 27 March 2017

References

1. Nienhueser IA, Qiu YM (2016) Economic and environmental impacts of providing renewable energy for electric vehicle charging—a choice experiment study. Appl Energ 180:256–8
2. Islam MM, Pandey AK, Hasanuzzaman M, Rahim NA (2016) Recent progresses and achievements in photovoltaic-phase change material technology: a review with special treatment on photovoltaic thermal-phase change material systems. Energ Convers Manage 126:177–204
3. Hemmati R, Saboori H (2016) Emergence of hybrid energy storage systems in renewable energy and transport applications—a review. Renew Sust Energ Rev 65:11–23
4. Guo J, Zhou WH, Pei YL, Tian QW, Kou DX, Zhou ZJ, Meng YN, Wu SX (2016) High efficiency CZTSSe thin film solar cells from pure element solution: a study of additional Sn complement. Sol Energy Mater Sol Cells 155:209–15
5. Han JF, Jian Y, He Y, Liu YN, Xiong XL, Cha LM, Krishnakumar V, Schimper HJ (2016) Nanostructures of CdS thin films prepared by various technologies for thin film solar cells. Mater Lett 177:5–8
6. Paez DJ, Huante-Ceron E, Knights AP (2016) Indium as a p-type dopant of thin film silicon solar cells. Thin Solid Films 615:358–65
7. Jovanov V, Xu X, Shrestha S, Schulte M, Hupkes J, Zeman M, Knipp D (2013) Influence of interface morphologies on amorphous silicon thin film solar cells prepared on randomly textured substrates. Sol Energy Mater Sol Cells 112:182–9
8. Zhang T, Zhang P, Li SB, Li W, Wu ZM, Jiang YD (2013) Black silicon with self-leaning surface prepared by wetting processes. Nanoscale Res Lett 8:351
9. Chen YH, Liu YH, Huang CF, Liu JC, Lin CC (2015) Improved photovoltaic properties of amorphous silicon thin-film solar cells with an un-doped silicon oxide layer. Mater Sci Semicond Process 31:184–8
10. Liu K, Yao WH, Wang DY, Ba D, Liu HL, Gu XG, Meng DH, Du GY, Xie YH, Ba YS (2016) A study of intrinsic amorphous silicon thin film deposited on flexible polymer substrates by magnetron sputtering. J Non-Cryst Solids 449:125–32
11. Li SB, Wu ZM, Jiang YD, Li W, Liao NM, Yu JS (2008) Structure and 1/f noise of boron doped polymorphous silicon films. Nanotechnology 19:085706
12. Fortes M, Comesana E, Rodriguez JA, Otero P, Garcia-Loureiro AJ (2014) Impact of series and shunt resistances in amorphous silicon thin film solar cells. Sol Energy 100:114–23
13. Li SB, Jiang YD, Wu ZM, Wu J, Ying ZH, Wang ZM, Li W, Salamo G (2011) Origins of 1/f noise in nanostructure inclusion polymorphous silicon films. Nanoscale Res Lett 6:281
14. Wang GH, Shi CY, Zhao L, Diao HW, Wang WJ (2016) Fabrication of amorphous silicon–germanium thin film solar cell toward broadening long wavelength response. J Alloys Compd 658:543–7
15. Plentz J, Andra G, Pliewischkies T, Bruckner U, Eisenhawer B, Falk F (2016) Amorphous silicon thin-film solar cells on glass fiber textiles. Mater Sci Eng B 204:34–7
16. Steabler DL, Wronski CR (1977) Reversible conductivity changes in discharge-produced amorphous Si. Appl Phys Lett 31:292–4
17. Banerjee A, Guha S (1991) Study of back reflectors for amorphous silicon alloy solar cell application. J Appl Phys 69:1030–5
18. Carlson DE (1989) Amorphous-silicon solar cells. IEEE Trans Electr Devices 36:2775–80
19. Rech B, Wagner H (1999) Potential of amorphous silicon for solar cells. Appl Phys A 69:155–67
20. Bruggemann R, Kleider JP, Longeaud C, Mencaraglia D, Guillet J, Bouree JE, Niikura C (2000) Electronic properties of silicon thin films prepared by hot-wire chemical vapour deposition. J Non-Crys Sol 266–269:258–62
21. Zhou Y, Li X, Ren X, Yang L, Liu J (2014) Designing and fabricating double resonance substrate with metallic nanoparticles-metallic grating coupling system for highly intensified surface-enhanced Raman spectroscopy. Analyst 139:4799–805
22. Liu P, Yang SE, Ma YX, Lu XY, Jua YK, Ding D, Chen YS (2015) Design of Ag nanograting for broadband absorption enhancement in amorphous silicon thin film solar cells. Mater Sci Semicond Process 39:760–3

23. Zhang P, Li SB, Liu CH, Wei XB, Wu ZM, Jiang YD, Chen Z (2014) Near-infrared optical absorption enhanced in black silicon via Ag nanoparticle-induced localized surface plasmon. Nanoscale Res Lett 9:519
24. Tian BZ, Zheng XL, Kempa TJ, Fang Y, Yu NF, Yu GH, Huang JL, Lieber CM (2007) Coaxial silicon nanowires as solar cells and nanoelectronic power sources. Nature 449:885–9
25. Zhang J, Li J, Zheng LR, Lu YH, Moulin E, Haug FJ, Ballif C, Xu H, Dai N, Song WJ (2015) Simultaneous realization of light distribution and trapping in micromorph tandem solar cells using novel double-layered antireflection coatings. Sol Energy Mater Sol Cells 143:546–52
26. Deng C, Ki H (2016) Pulsed laser deposition of refractive-index-graded broadband antireflection coatings for silicon solar cells. Sol Energy Mater Sol Cells 147:37–45
27. Sachan R, Gonzalez C, Dyck O, Wu Y, Garcia H, Pennycook SJ, Rack PD, Duscher G, Kalyanaraman R (2012) Enhanced absorption in ultrathin Si by $NiSi_2$ nanoparticles. Nanomater Energy 2:11–9
28. Brahmi H, Ravipati S, Yarali M, Shervin S, Wang WJ, Ryou JH, Mavrokefalos A (2017) Electrical and optical properties of sub-10 nm nickel silicide films for silicon solar cells. J Phys D 50:035102
29. Hayzelden C, Batstone J (1993) Silicide formation and silicide-mediated crystallization of nickel-implanted amorphous silicon thin films. J Appl Phys 73:8279–89
30. Kelzenberg M, Boettcher S, Petykiewicz J, Turner-Evans D, Putnam M, Warren E, Spurgeon J, Briggs R, Lewis N, Atwater H (2010) Enhanced absorption and carrier collection in Si wire arrays for photovoltaic applications. Nat Mater 9:239–44